DECEMBER 1980 LRP 171/80

MICROPROCESSOR-CONTROLLED PHASE ANALYSIS

FOR A 2mm MICROWAVE INTERFEROMETER ON THE TCA TOKAMAK

J.B. Lister, R.W. Means, and P. Oberson

MICROPROCESSOR-CONTROLLED PHASE ANALYSIS FOR A 2mm MICROWAVE INTERFEROMETER ON THE TCA TOKAMAK

J.B. Lister, R.W. Means*, and P. Oberson

Centre de Recherches en Physique des Plasmas
Association Euratom - Confédération Suisse
Ecole Polytechnique Fédérale de Lausanne
CH - 1007 Lausanne / Switzerland

ABSTRACT

The phase analysis is presented for a 2mm microwave interferometer in use to measure the plasma density in a tokamak. Use is made of a Fast Phase Shifter constructed from a switchable four-part circulator to resolve the phase ambiguity inherent in a simple interferometer. The phase between 0 - 2π is calculated by a microprocessor accessing a look-up table and the total phase is calculated by taking the 0 to 2π crossings into consideration. It is software controlled and the complete sampling and analysis cycle takes 24 μseconds which is sufficiently rapid for the application considered. The phase information is available in analogue and digital form.

---

* Present address: Data / Ware Development
4204 Sorrento Valley Bld.
San Diego, CA 91121, USA

I. INTRODUCTION

The method of plasma density measurement by a microwave interferometer is a well-known diagnostic technique: the basic experimental arrangement is shown in Figure 1. The signal from the microwave source is split into two beams. One beam (the reference beam) is sent to the detector by means of waveguide and the other is transmitted through the plasma before being brought to the detector. In general, there will be a phase and amplitude difference between the two beams at the detector. Usually, the microwave frequency is well above the plasma frequency, ω_p; $\omega_p^2 = ne^2/m\,\varepsilon_o$ where n is the plasma electron density, e is the electron charge, m is the electron mass, and ε_o is the permittivity of free space. The units are MKS. The attenuation of the beam in the plasma is usually negligible. However, the plasma causes a phase shift in the beam due to the change in refractive index of the medium. The phase shift ϕ is related to the density of the plasma by[1]

$$\phi = \int dx \, \frac{2\pi}{\lambda_o} \left\{ 1 - \sqrt{\frac{n(x)}{n_c}} \right\} \qquad (1)$$

where λ_o is the free space microwave wavelength, n(x) is the plasma electron density along the path length and n_c is the critical density corresponding to a plasma with ω_p equal to the microwave frequency, ω_o, i.e. $\omega_o^2 = n_c e^2/m\,\varepsilon_o$. If the plasma density is much less than the critical density then equation (1) becomes approximately

$$\phi = \frac{e^2}{2\,\varepsilon_o mc\,\omega_o} \int n(x)dx \qquad (2)$$

In general, the signal which comes from the detector contains a varying component which is proportional to the sine or cosine of the phase. In many experiments, the plasma density is pulsed in time so that the phase shift ϕ is a function of time. A typical experimental problem is to measure the electron density during a tokamak discharge which may last between several milliseconds and several seconds. Given a line density, ($\int n(x)dx$), shown in Figure 2a, we have a phase ϕ shown in Figure 2b, and a detector signal, S, as shown in Figure 2c. Experimentally we have only the detector signal, S, and from this the phase and the line density must be deduced. A major problem with such an interferometer is that the decoding from the detector signal to the phase not unique. At each peak of sinϕ ($\phi = \frac{(2n+1)\pi}{2}$, n = 0,1,2...) the density change could have reversed direction and the sine of the phase would be the same; i.e., since $\sin(\frac{\pi}{2} + \delta) = \sin(\frac{\pi}{2} - \delta)$, there is an ambiguity in determining the phase from the trace in Figure 2c after each peak in the detector signal.

This ambiguity is usually resolved by sweeping the frequency of the microwave source many times during the tokamak pulse. This technique gives a display on an oscilloscope known as zebra striping.[1] Another method which eliminates the ambiguity is shown in Figure 3. There are two reference beams split off from the source and brought to separate detectors; the transmitted beam is also split into two beams. Thus if we arrange the reference beams to have a constant relative phase offset of $\pi/2$, the one detector signal will be proportional to the sine of ϕ and the other signal will be proportional to cosine of ϕ. The two signals now allow an unambiguous interpretation of the density behaviour. In other words, at those places near $\pi/2$ where $\sin(\pi/2 + \delta) = \sin(\pi/2 - \delta)$, the cosine signal gives a direction to the phase change since $\cos(\pi/2 + \delta) = -\cos(\pi/2 - \delta)$.

The solution shown in Figure 3 is usually an expensive solution in terms of microwave hardware. A better solution is shown in Figure 4. The item labeled FPS is a fast phase shifter which can shift the phase by $\pi/2$ much faster than the change in electron density. We now have a chopped signal from the detector, of which one part is proportional to the sine of ϕ and the other is proportional to the cosine of ϕ. A fast phase shifter can be much cheaper than the complete second beam alternative shown in Figure 3. The signal processing is only slightly more complex, and the signal level at the detector is higher.

The disadvantages of the zebra-striping method are the need to frequency modulate the signal and the difficulty of real time signal analysis if the density is required as a feedback or control parameter. On the other hand, the system shown in Figure 4 does not need a frequency modulated source and is easily analyzed in real time.

The schematic of the signal processing is shown in Figure 5. The sine of ϕ and the cosine of ϕ give an unambiguous determination of ϕ (between 0 and 2π). This is accomplished by digitizing the two signals and using a microprocessor to look up the corresponding value of ϕ in a table stored in Read Only Memory. Branch cut crossings from 0 to 2π and from 2π to 0 can be kept track of digitally by the microprocessor and $\phi(t)$ can be computed in real time.

The realization of our interferometer shown schematically in Figure 4 is shown in more detail in Figure 6. The source is a Gunn oscillator built by TRG at 46.6 GHz working into a frequency tripler which gives nearly 10 milliwatts at 140 GHz. Fast phase shifters are not yet available in this frequency band. Instead a switchable 4-port circulator has been used to achieve the same result. This unit can be switched in 5 µs so that either the signal goes from port 1 to port 2 or from port 1 to port 4. The equivalent of a $\pi/2$ phase shift is the circulator switched so that the signal goes from port 1 to port 4, where it encounters a short circuit which reflects the signal back to port 3. There it encounters a tunable short and is reflected back to port 2. It has thus travelled a path different from that of the unswitched signal and arrives at port 2 with a different phase (and amplitude). The phase shift is adjustable to $\pi/2$ by the tunable short.

Let us consider in more detail the signal which arrives at the detector. In Figure 6 the reference beam and the plasma beam are combined in a hybrid ring which has a detector at the summing port and one at the difference port. The reference beam has an amplitude

$$E_R = A \cos \left[\omega_o t + \phi_R + P(t)\pi/2 \right] \qquad (3)$$

where A is the amplitude of the electric field, ω_o is the microwave frequency, ϕ_R is the phase of the reference beam and $P(t)\,\pi/2$ is the switchable phase shift.

The plasma beam has an amplitude

$$E_P = B \cos(\omega_o t + \phi_P + \phi) \qquad (4)$$

where B is the amplitude of the electric field, ϕ_P is the phase of the plasma beam and ϕ is the phase shift due to the plasma given by equation (1). The detectors at the sum and difference ports of the hybrid ring perform a squaring and time average over the microwave frequency to give

$$S(t) = \langle (E_R + E_P)^2 \rangle \qquad (5)$$

$$D(t) = \langle (E_R - E_P)^2 \rangle \qquad (6)$$

Thus

$$S(t) = \frac{A^2+B^2}{2} + AB\cos(\phi_R - \phi_P - \phi + P(t)\pi/2) \qquad (7)$$

$$D(t) = \frac{A^2+B^2}{2} - AB\cos(\phi_R - \phi_P - \phi + P(t)\pi/2) \qquad (8)$$

The signals S and D are then subtracted by a differential amplifier and the result is

$$S(t)-D(t) = 2AB\cos(\phi_R - \phi_P - \phi + P(t)\pi/2) \qquad (9)$$

The constant phase difference $\phi_R - \phi_P$ can be zeroed or more simply measured at $t = 0$ and compensated for in the microprocessor program. The switch function $P(t)$ is also controlled by the microprocessor with a fixed period of 64 microseconds. When $P = 0$ the signal $(S(t) - D(t)$ is sampled, digitized and stored in memory. When $P = 1$, 32 microseconds later, the signal is again sampled, digitized and stored. Seven bits of the A/D converters are used. The two seven bit words representing the cosine and sine of the phase shift are then used as a 14-bit address for a 16 K ROM table to look up the value of ϕ. The microprocessor software to accomplish this and to count the branch cut crossings is shown in Fig. 7 and was encoded for a Motorola 6800. The software takes 64 cycles to execute and thus the basic data sampling is done every 64 microseconds for a one MHz microprocessor clock. If the phase shift ϕ changes by more than π in 64 μs then the microprocessor will begin to make errors in the total phase. This represents an upper limit to the experimental rate of change of density that is reliably measurable. For the tokamak for which this system was designed this limit is $3.4 \cdot 10^{16}$ electrodes/cm^3. sec at the center of the plasma. This limit was above the expected rate of change. The final output of the microprocessor consists of two analog signals in real time proportional to $\phi(t)$ (12 bits) and $\phi(t)$ reduced to $0 - 2\pi$ radians (8 bits). These signals are delayed by the cycle time of the software (64 μs), which is insignificant for our application.

II. OPERATION OF THE MICROWAVE CIRCUIT

The microwave interferometer circuit was set up using a rotating wedge-sectioned disk made out of perspex placed in the "plasma" arm to produce a time varying phase. The antenna spacing was the same as in the tokamak experiment. We found that the antenna gain pattern efficiency for open-ended X-band waveguides was more favorable at this antenna spacing (520 mm) than the antenna patterns from true fundamental horns. Initial testing was performed using a straight waveguide section in place of the phase shift circulator and considerable setting up problems were encountered. However, the interferometer worked as expected with smooth fringes obtained at the relatively slow phase change rate produced by the rotating disk. Setting up the diodes on the hybrid-ring was not straight forward as the diode mount stub and the two E-H tuner stubs had to be optimized for the summing port and difference port of the hybrid-ring. A considerable amount of power was reflected from each one as evidenced by the effect on one diode signal of slightly detuning the other diode assembly. Nonetheless, even with an abundance of reflected power, the interferometer worked well.

With the phase shift circulator in place in the circuit, we had, in principle, one more device to adjust, namely the stub tuner which varies the phase of the signal reflected from port number 4 (Fig. 6). We found that the reflection from the diodes caused considerable confusion of the two signals obtained with the circulator ON and OFF. With the circulator OFF we obtained results similar to those without the circulator present, as was expected. With the circulator ON, the power transmitted through the circulator should be reduced by 4 dB. In reality, the ON signal was of a similar magnitude to the OFF signal. A further observation was that with the circulator OFF, the diode signals were sensitive to the port 4 stub-tuner phase. These observations are all consistent with the presence of a significant amount of power reflected from the diodes. This is a known problem but the simple standard solution, which is to place an attenuator before each diode, was not acceptable to us since we are running with a low power source. However, we found that by judicious adjustment of all the various tunable elements we were able to obtain a circulator ON signal which was very close to a phase-shift of 90° from the circulator OFF signal. In fact, the presence of the reflected power, by increasing the diode signals in the ON case, could be considered to have at least one advantage. The main disadvantage was the difficulty in obtaining and reproducing this 90° phase shift. The oscilloscope traces obtained are shown in Fig. 8.

III. OPERATION OF THE MICROPROCESSOR UNIT

The signals Σ - Δ obtained with circulator ON and OFF respectively are treated as in Fig. 5. The raw signals have a DC offset due to the fact that the microwave circuit is not ideal, and also have different amplitudes. Both offset and gain are adjusted in the unit to give equal amplitude symmetrical signals. The 8-bit and 12-bit outputs are shown in Fig. 8 for the phase changes produced by the rotating disk. We see from these curves that there is an S-shaped distortion, and this is due to the fact that the Y signal is not simply a phase-shifted copy of X, but a complicated distortion of it. However, if we plot the error in phase for a complete cycle (Fig. 9), we find a maximum error of 30°, corresponding to a typical peak plasma density error of 0.04 $10^{13}/cm^3$ which is negligible from the experimentalist's viewpoint.

In order to reduce the noise on ϕ to a minimum, the diode signal is filtered by a simple RC circuit (Fig. 10). Furthermore a filter was installed between the Sample and Hold Module and the ADC. In this way the demultiplexed signal could be filtered down to the highest true fringe frequency, which increased the signal-to-noise ratio considerably.

IV. RESULTS DURING TOKAMAK OPERATION

The interferometer described was constructed for use on the TCA tokamak,[2] characterized by a major radius of 0.61 m, a minor diameter of 0.34 m along which the plasma density is to be measured and peak electron densities $n_e(0) < 7 \times 10^{19} m^{-3}$. The fast varying magnetic fields used to create a plasma discharge had to be carefully screened from the 4-port circulator, a sensitive ferrite device, and from the high impedance pre-amplifier circuit.

The operation of the interferometer during a tokamak plasma discharge suffered from two main problems. First, there was the question of the rate of change of plasma density, or phase change rate. The algorithm in the software to decide whether the density is rising or falling was to choose the least density change per sample period. Thus if the density changes by $\pi + \delta$ a change of $-\pi + \delta$ will be assumed, and a change of π per cycle is the theoretical maximum for a perfect system. The non-linearity of the calculated phase reduces this below π and an inherent noise will reduce it still further. The maximum phase change per cycle will then be π-(Maximum noise) - (Maximum distortion error). This figure appears to be about 180° - 30° - 45° giving 105°/cycle or 4.6 fringes/msec. This figure is not as far above the experimental maximum values obtained as had been hoped.

Secondly, the plasma column is cylindrical and we aim to measure along a diameter (Fig. 6). During the first few milliseconds of a tokamak discharge, the rate of change of density (phase) is at its maximum and the plasma is at its least stable in position. During these milliseconds the plasma column will displace itself outwards and back and the probing beam will not always be along a diameter. At this time, there is also a reduction in signal amplitude due to refraction of the beam and an increase in genuine rapid phase variation. Both these effects reduce the maximum interpretable rate of change of density from that calculated above. At the end of the tokamak discharge the rate of decrease in density is also fast and the position is also less stable. During a disruption in the plasma discharge, the total phase is lost in almost all cases.

As a result of both of these problems, the absolute phase can suffer one or more errors during a tokamak discharge. The central part of the pulse (5-80 msec typically) remains smooth and the density variation is faithfully reproduced. The fact that phase information can be lost at both ends of the cycle precludes us from inferring the errors during build-up. Two typical traces are shown in Fig. 11 one of which follows the density as a function of time, and the other of which has obvious jumps of 2π radians.

V. IMPROVED VERSION

If we assume that the only source of trouble is the slow (64 μsec) cycle rate then we must decrease the cycle time. On the other hand, such a decrease also decreases the filtering time and at a certain juncture the diode or even plasma noise may dominate.

The first speed increase was obtained very simply be increasing the microprocessor clock rate from 1 MHz to 1.5 MHz, reducing the cycle time from 64 μsec to 43 μsec. This was possible without changing the ROM in which the phase look-up table was stored.

The second speed increase was obtained by replacing part of the software cycle by hardware. This was performed on the logic which determined whether the number of fringes had increased or decreased. The reduced software shown in Figure 7 corresponded to 26 out of 64 cycles. This reduced the cycle time to 37 μsec, or to 25 μsec with both increases in speed installed. The filtering was reduced correspondingly and remained acceptable. The timing cycle of the circulator was adjusted and the new system was tested on real tokamak discharges.

A considerable improvement was found and density rises of up to 4.5 fringes/msec were handled correctly. Above this rate of increase of density, fringes were still lost but the distortion in phase was the dominant effect. Careful adjustment of the complete system was required and the capability of the decoding matched the typical plasma performance.

VI. CONCLUSIONS

The evaluation of total phase change of the 2mm interferometer during typical tokamak discharges has been successfully achieved by a microprocessor-controlled phase analyser and a fast phase switcher. The cycle rate of the phase analyser had to be increased to cater for the rapid phase shifts at the beginning of a tokamak discharge. Part of this increase in speed was achieved by hardwiring some of the software. The use of a 4-port-circulator as a fast phase shifter was successful, but the implementation of this microwave hardware was greatly hindered by spurious reflections.

ACKNOWLEDGMENTS

We thank Mr. Perotti for constructing the circulator driver and diode amplifier and Mr. Simik for providing the basic microprocessor hardware.

This work was supported by the Swiss National Science Foundation and by Euratom.

FIGURES

REFERENCES

[1] G.B. Wharton, Microwave Diagnostic for Controlled Fusion Research UCRL 4836 (1957).

TFR Group, Nuclear Fusion 18, 5 (1978).

[2] A.D. Cheetham et al., Design and Construction of the TCA Tokamak. Symposium on Fusion Technology, Oxford (1980).

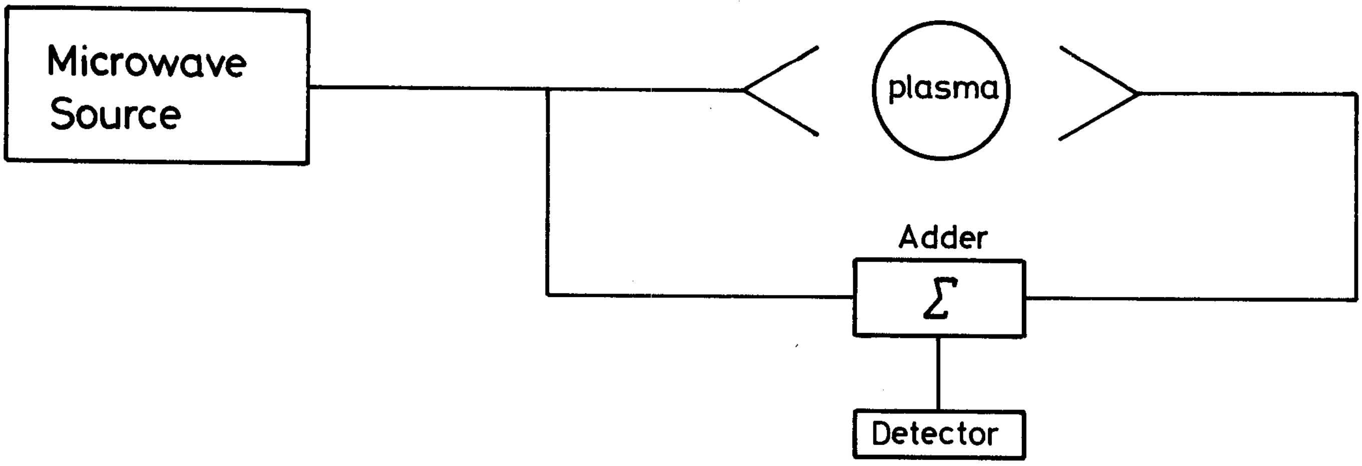
Microwave Source
plasma
Adder
Σ
Detector

Fig. 1

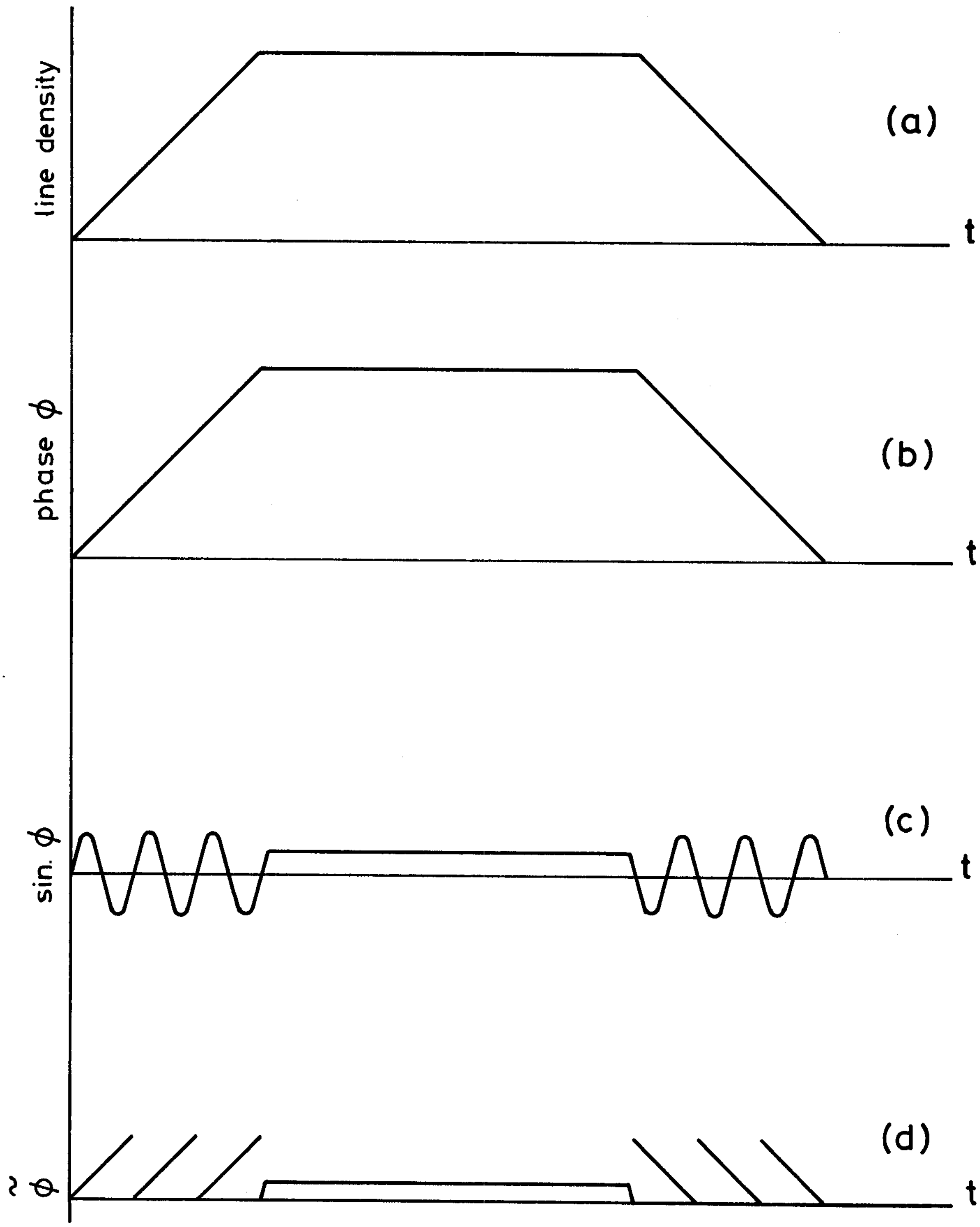
line density
(a)
t
phase φ
(b)
t
sin. φ
(c)
t
~ φ
(d)
t

Fig. 2

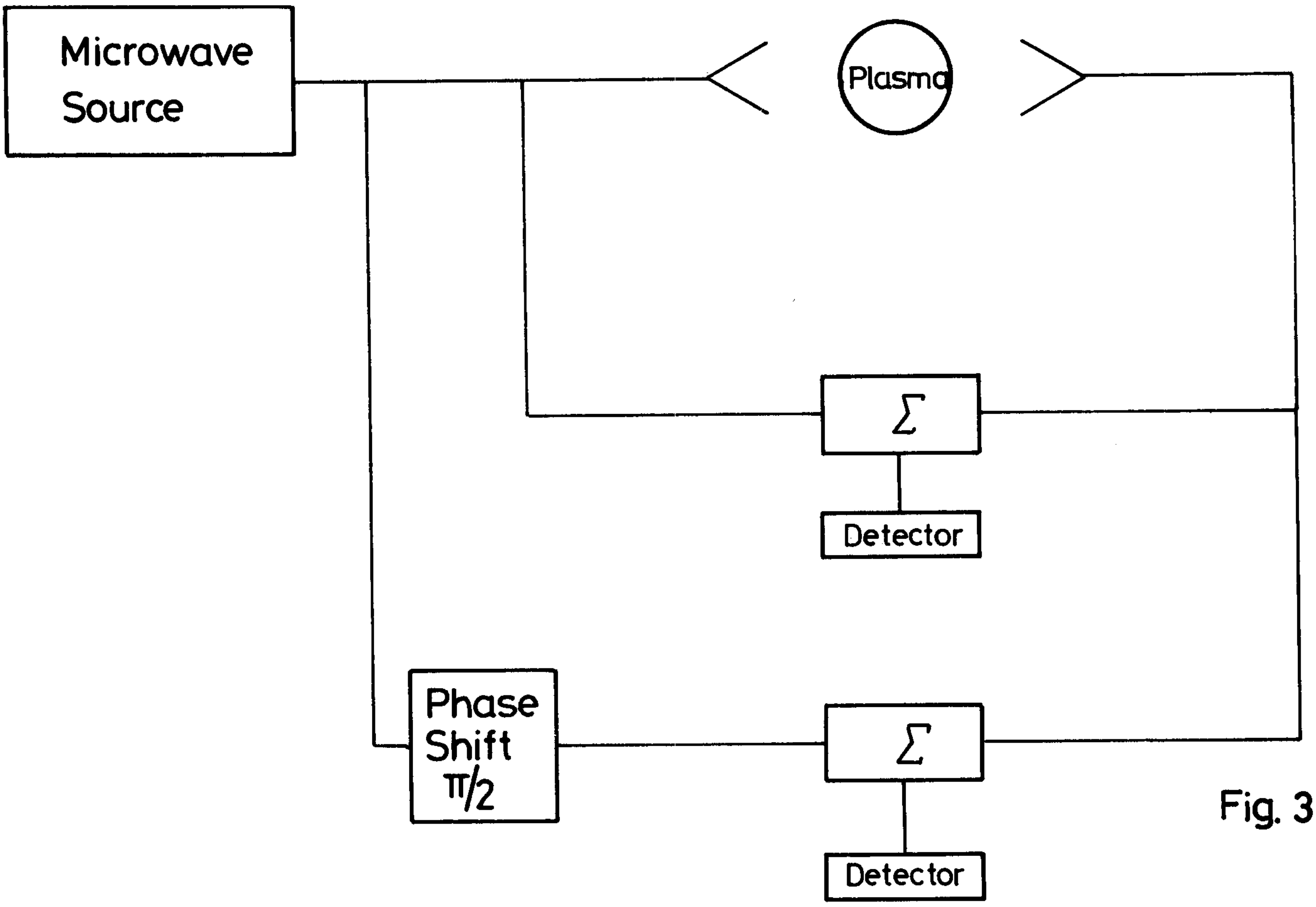
Microwave Source
Plasma
Σ
Detector
Phase Shift π/2
Σ
Detector

Fig. 3

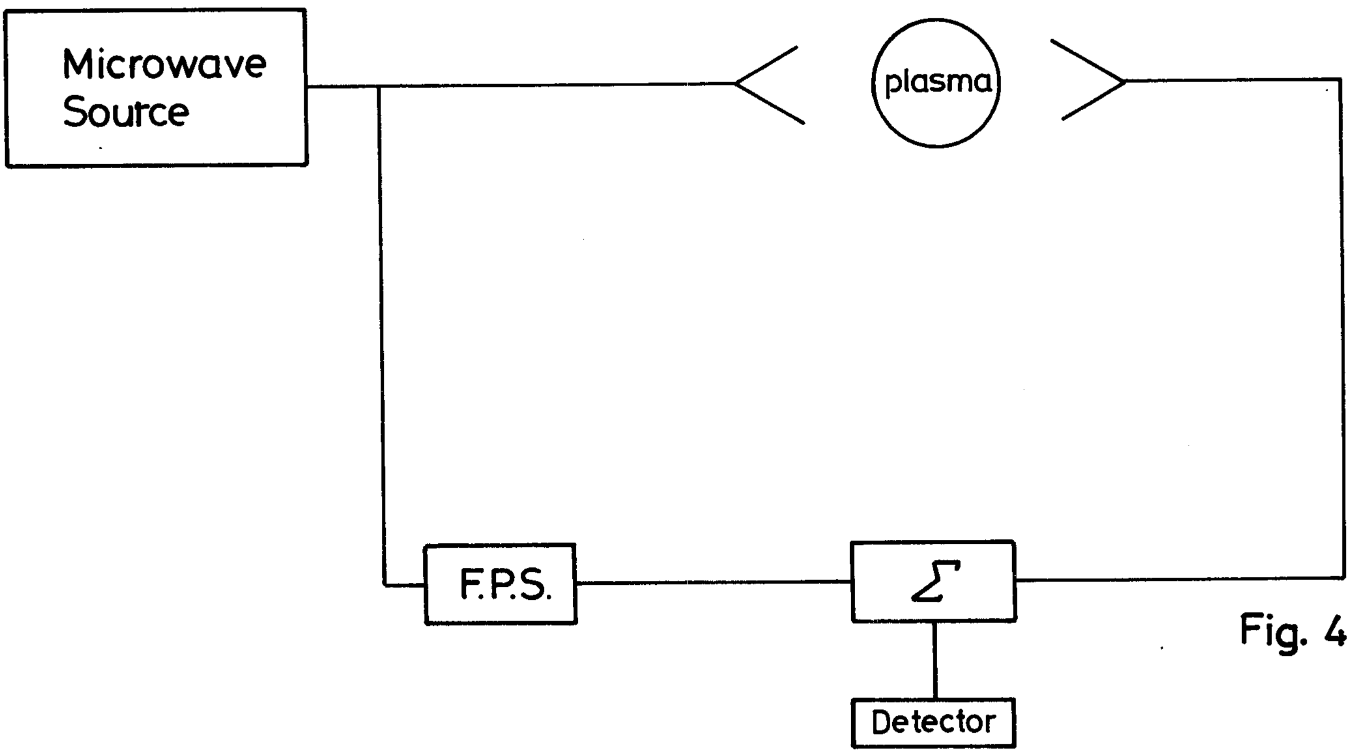
Microwave Source
plasma
F.P.S.
Σ
Detector

Fig. 4

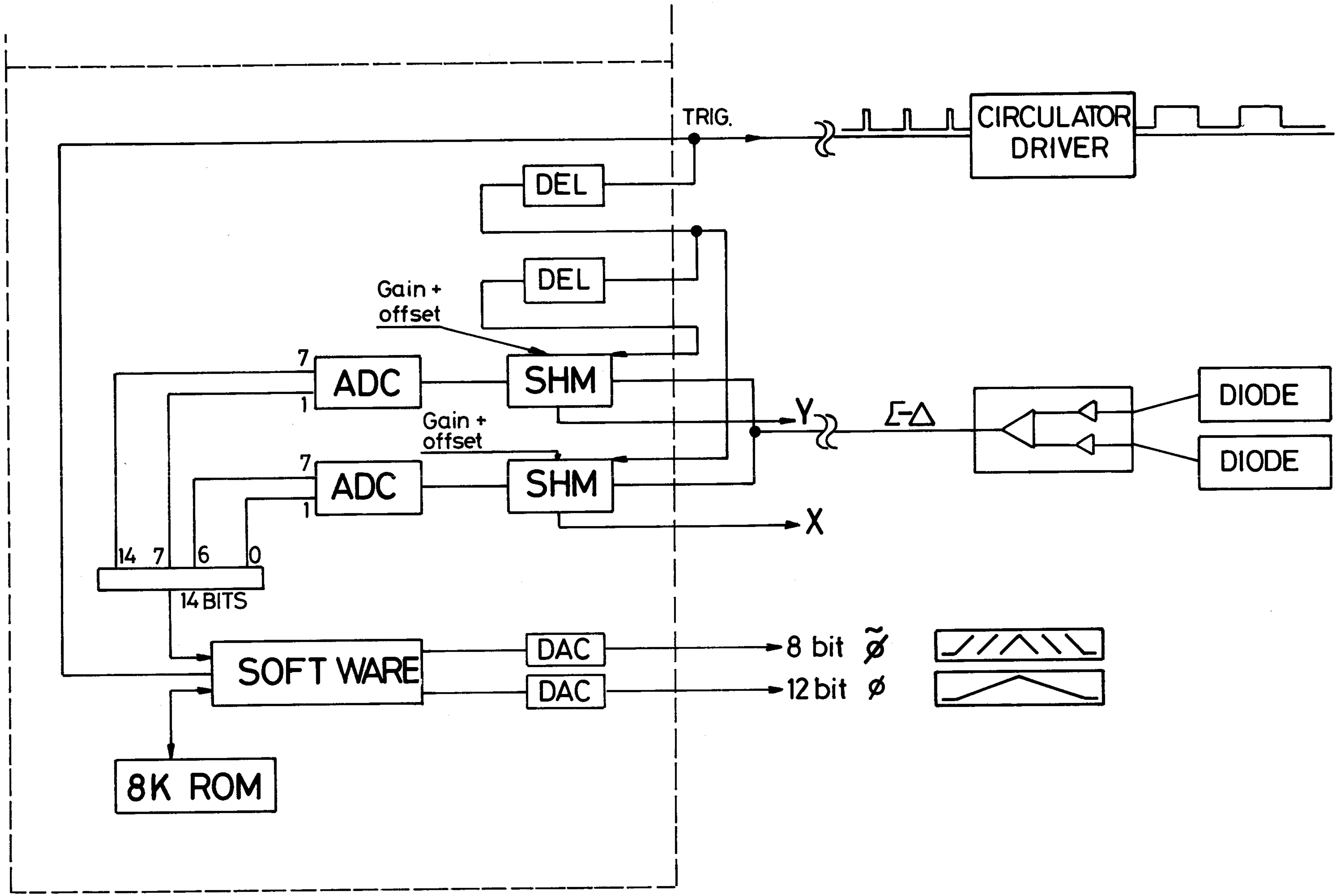
TRIG.
CIRCULATOR DRIVER
DEL
DEL
Gain + offset
Gain + offset
ADC
ADC
SHM
SHM
7
1
7
1
14
7
6
0
14 BITS
Y
X
Σ-Δ
DIODE
DIODE
SOFT WARE
DAC
DAC
8 bit $\tilde{\phi}$
12 bit ϕ
8K ROM

Fig. 5

Fig. 6

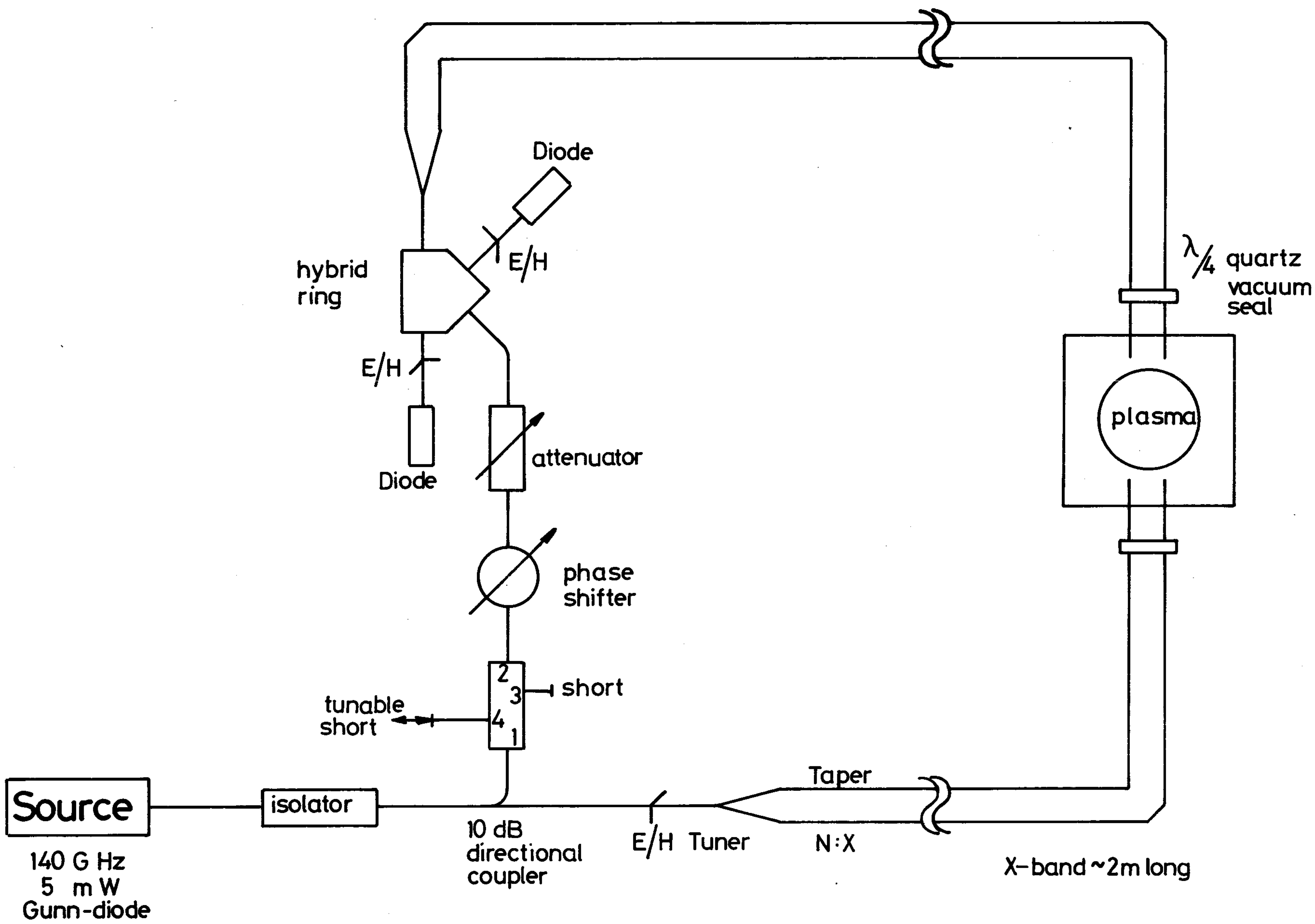

Diode
E/H
hybrid ring
E/H
Diode
attenuator
phase shifter
short
tunable short
2
3
4
1
Source
140 G Hz
5 mW
Gunn-diode
isolator
10 dB directional coupler
E/H
Tuner
Taper
N:X
X-band ~2m long
λ/4 quartz vacuum seal
plasma

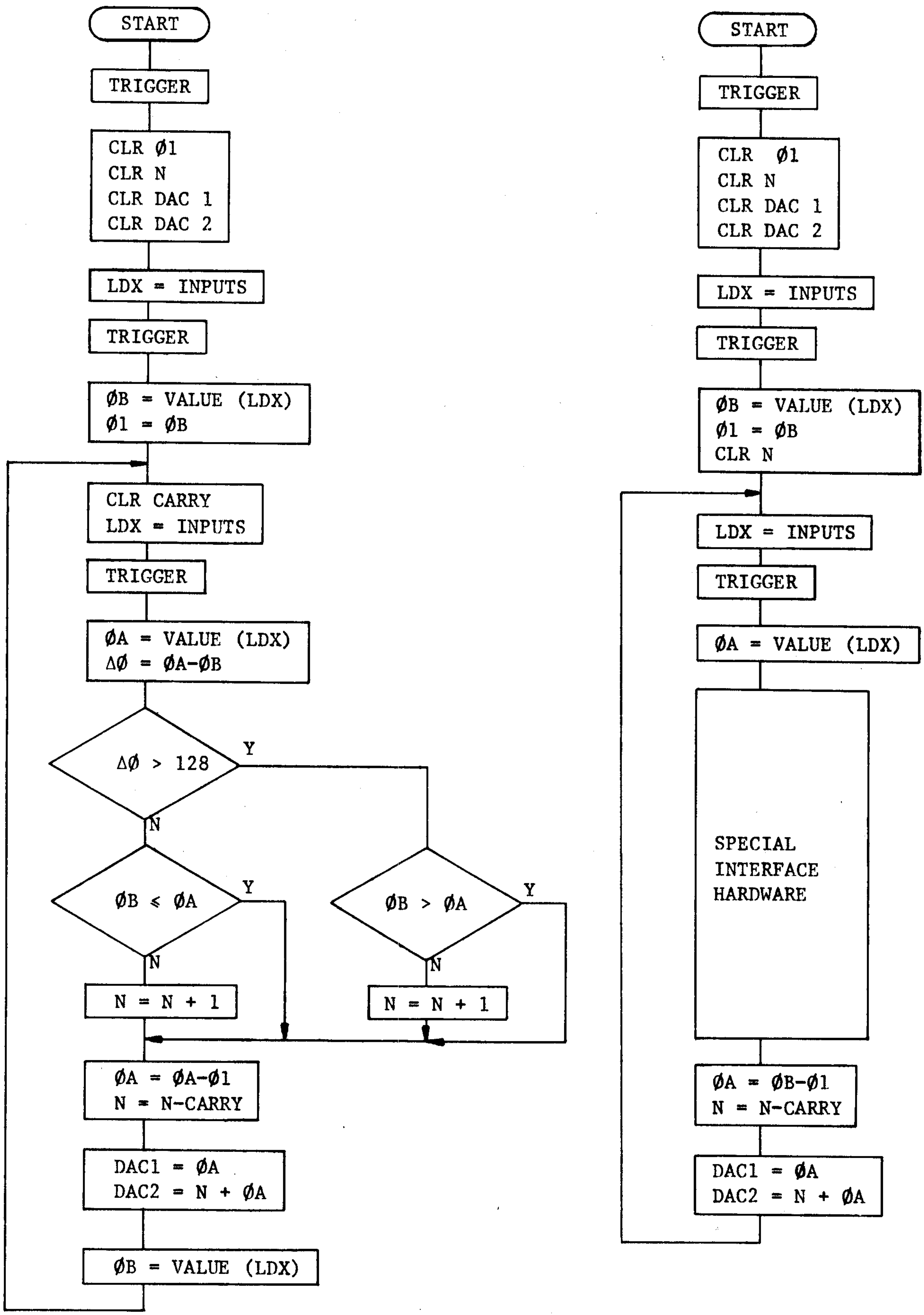

START
TRIGGER
CLR Ø1
CLR N
CLR DAC 1
CLR DAC 2
LDX = INPUTS
TRIGGER
ØB = VALUE (LDX)
Ø1 = ØB
CLR CARRY
LDX = INPUTS
TRIGGER
ØA = VALUE (LDX)
ΔØ = ØA-ØB
ΔØ > 128
Y
N
ØB ⩽ ØA
Y
N
ØB > ØA
Y
N
N = N + 1
N = N + 1
ØA = ØA-Ø1
N = N-CARRY
DAC1 = ØA
DAC2 = N + ØA
ØB = VALUE (LDX)
START
TRIGGER
CLR Ø1
CLR N
CLR DAC 1
CLR DAC 2
LDX = INPUTS
TRIGGER
ØB = VALUE (LDX)
Ø1 = ØB
CLR N
LDX = INPUTS
TRIGGER
ØA = VALUE (LDX)
SPECIAL
INTERFACE
HARDWARE
ØA = ØB-Ø1
N = N-CARRY
DAC1 = ØA
DAC2 = N + ØA

Fig. 7

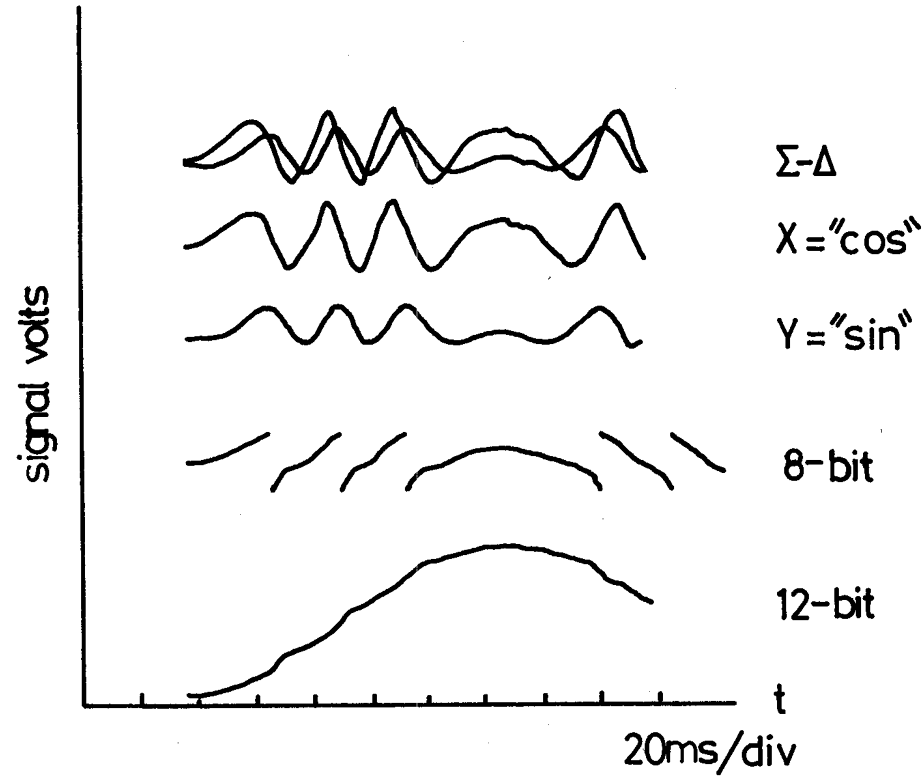

Fig. 8

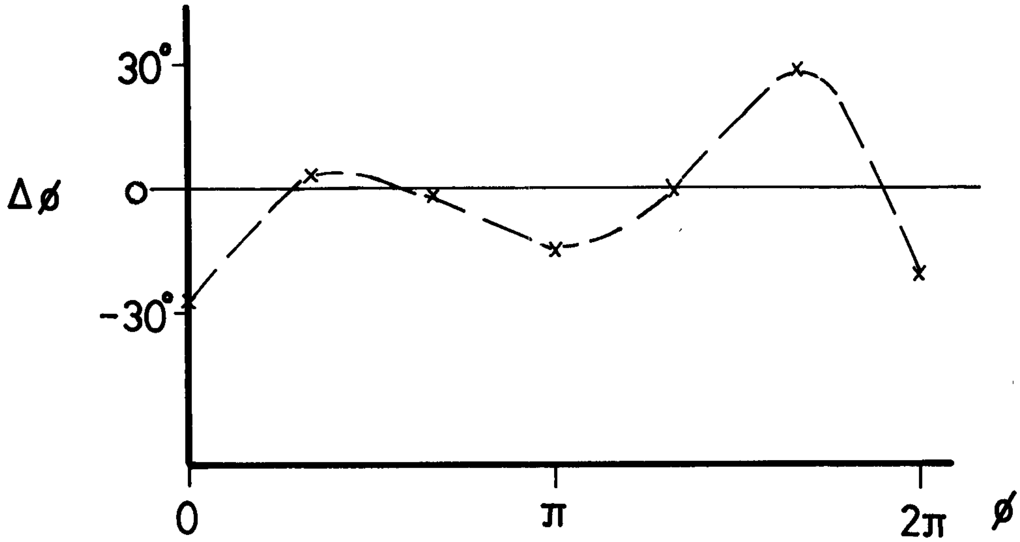

Fig. 9

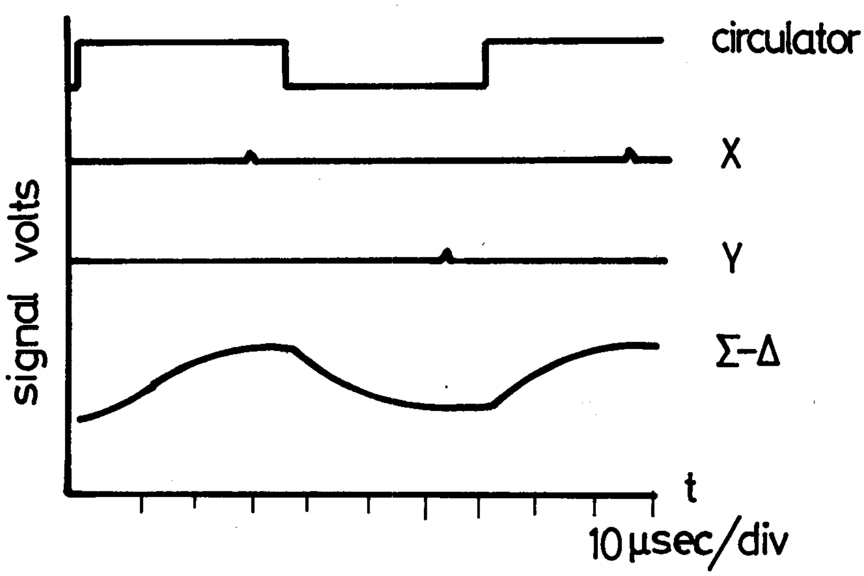

Fig. 10

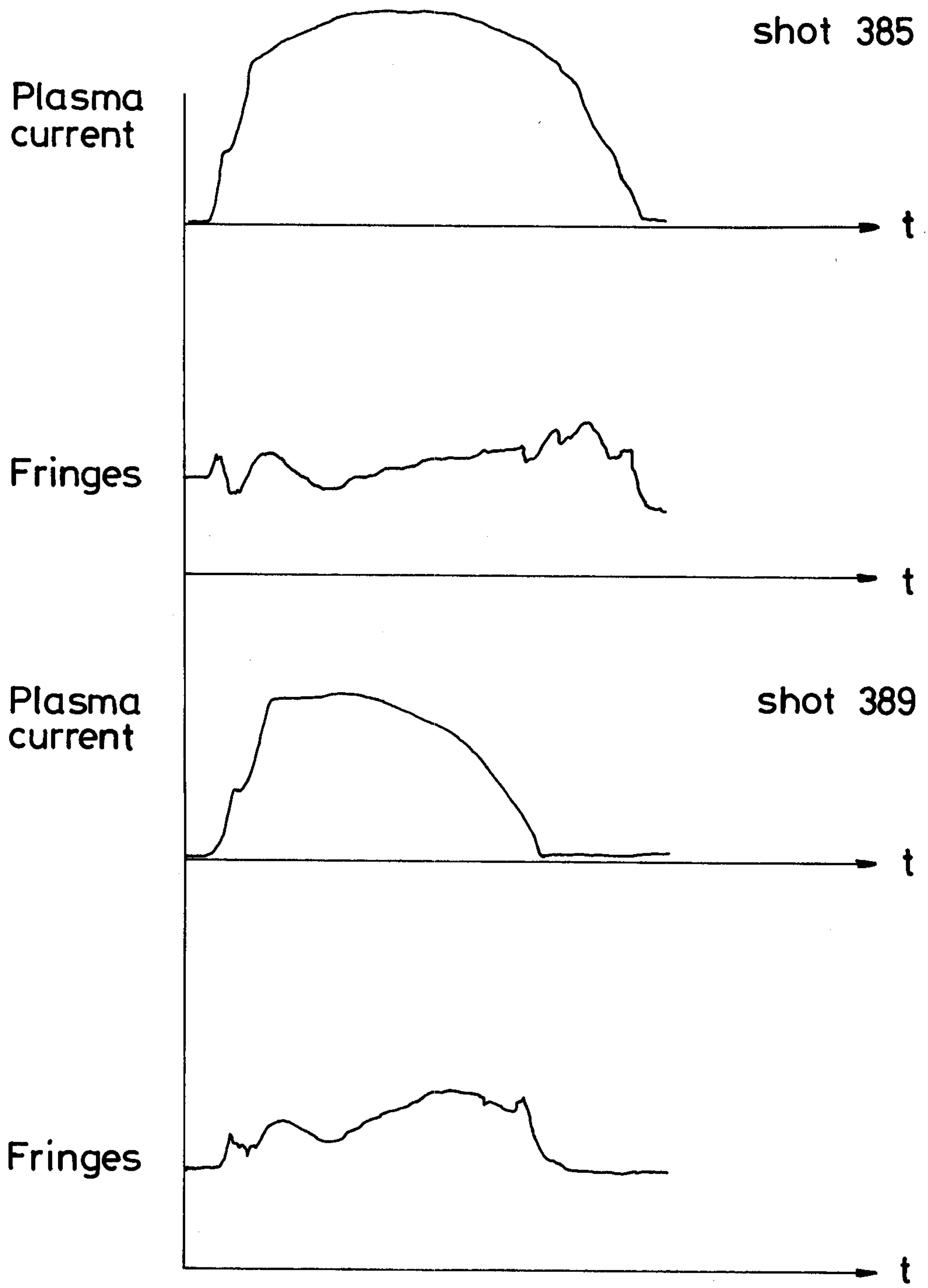
shot 385
Plasma current
t
Fringes
t
Plasma current
shot 389
t
Fringes
t

Fig. 11